TEMPERATURE FIELDS IN SWELLING MATERIALS

V. L. Strakhov and N. G. Chubakov

UDC 536.416:541.64

A method is outlined for calculating the nonsteady temperature fields in polymer materials swelling on heating and passing through a plastic state in the region of thermal decomposition.

With the action of heat on polymer materials (PM) at a definite pressure of the surrounding medium, the phenomenon of swelling is observed. The reason for this is the presence of a plastic (viscofluid) state and gas liberation in the region of thermal decomposition of the PM. The pressure of the gaseous products of thermal decomposition leads to extension of the plastic body of the porous decomposition region. On account of the swelling, the temperature field in the material is distorted, and its heating depth is reduced. Similar phenomena are observed in the heating of certain materials used in fireproofing (systems based on foaming paint and varnish coatings).

The results of investigating [1] temperature fields in PM in the presence of zones of reacting material and pyrolysis of the initial material, and when the dependence of the thermophysical characteristics on the temperature and porosity is taken into account, are known. PM deformation (on account of swelling) and the associated significant (as shown below) changes in the nonmechanical parameters have not previously been considered.

The mathematical model of the nonsteady heating of a swelling PM together with the traditional conservation equations for the energy, mass of the material, motion, diffusion, and the equation of state of the gaseous thermal-decomposition products [2], includes the equations of polymer mechanics: the equation of motion of the body of the porous region of thermal decomposition, and geometric and physical equations (rheological equations of state). The system of equations for calculating the temperature fields in swelling PM is obtained under the following assumptions.

1. Heat and mass transfer along the working (heated) surface of the material is negligibly small in comparison with transfer in the perpendicular direction.

2. Deformation of the body of the porous plastic region is one-dimensional.

3. Motion of the body and the volatiles in the pores is quasisteady.

4. Diffusional mass flows are negligibly small in comparison with the convective flows.

The basis for assumption 1 is that, in the great majority of cases that are of practical importance, the gradients of the heat and mass fluxes along the surface of the material are negligibly small in comparison with the transverse fluxes. Assumption 2 is correct in view of the small thickness of the plastic region (fractions of a mm) in comparison with its extent in the plane parallel to the working surface of the material. Assumptions 3 and 4 are confirmed by numerical estimates of the order of magnitude of the corresponding terms in the equations of motion and diffusion. Taking account of these assumptions, the system takes the form

$$\rho^{0\mathrm{I}} c_p^{\mathrm{I}} (1-\Pi)\frac{\partial T}{\partial t} = \frac{\partial}{\partial \xi}\left(\lambda_\Sigma \frac{\partial T}{\partial \xi}\right) + [\rho^{0\mathrm{I}} c_p^{\mathrm{I}} (1-\Pi)(v^x - v_S^{\mathrm{I}} + v^{\mathrm{I}}) + c_p^{\mathrm{II}} G]\frac{\partial T}{\partial \xi} - \rho_0 (1-K) Q_\Sigma \frac{\partial}{\partial t}\left(\frac{\chi}{1+\varepsilon}\right), \quad \xi = y - y_S(t), \tag{1}$$

$$\frac{\partial \rho^{\mathrm{II}} \Pi}{\partial t} + \frac{\partial \rho^{\mathrm{II}} \Pi v^{\mathrm{II}}}{\partial y} = \rho_0 (1-K)\frac{\partial}{\partial t}\left(\frac{\chi}{1+\varepsilon}\right), \tag{2}$$

Translated from Inzhenerno-Fizicheskii Zhurnal, Vol. 45, No. 3, pp. 472-479, September, 1983. Original article submitted June 4, 1982.

0022-0841/83/4503-1054$07.50

$$\frac{\partial p}{\partial y} = -\frac{\Pi\mu^{II}}{k}(v^{II} - v^{I}), \tag{3}$$

$$p = \frac{\rho^{II} RT}{M}, \tag{4}$$

$$\frac{\partial (1-\Pi)\sigma_y}{\partial y} - p\frac{\partial \Pi}{\partial y} - F = -\frac{\Pi^2\mu^{II}}{k}(v^{II} - v^{I}), \tag{5}$$

$$\frac{\partial l}{\partial y} = \ln(1+\varepsilon_y), \quad \frac{\partial l}{\partial t} = v^{I} = \int_{y_{BP}}^{y} \frac{1}{1+\varepsilon_y}\frac{\partial \varepsilon_y}{\partial t}\,dy, \quad v_S^{I} = v_{EP}^{I}, \tag{6}$$

$$\varepsilon_y = A_\varepsilon \sigma_y^{\beta} t_*^{r} \exp(-B_\varepsilon/T), \quad \varepsilon = \frac{\ln(1+\varepsilon_y)}{1-\ln(1+\varepsilon_y)}, \quad t_* = t - t_{BP}. \tag{7}$$

The boundary conditions are

$$T|_{t=0} = T_0(\xi), \tag{8}$$

$$-\lambda_\Sigma \frac{\partial T}{\partial y}\bigg|_{y=y_S} = \left(\frac{\alpha}{c_p^{II}} - \eta G_S\right)(I_e - I_S) + A_{ef}\sigma'(T_e^4 - T_S^4) + G^{ch}Q_S^{ch}, \tag{9}$$

$$-\lambda_L \frac{\partial T}{\partial y}\bigg|_{y=L} = \frac{\alpha_L}{c_p^{II}}(I_{eL} - I_{SL}), \quad M_e = v_e/a, \tag{10}$$

$$\mathrm{Nu} = 0{,}0296\,\mathrm{Re}_S^{0,8}\,\mathrm{Pr}_S^{0,46}(1 + 0{,}2\,\mathrm{Pr}_S^{0,33}M_e^2)^{0,11}, \quad G^{ch} = \frac{\alpha b}{(1-\Pi)(1-\eta_M)c_p^{I}}\left(\frac{K}{K - m_F}\right), \tag{11}$$

$$\lambda_{\Sigma s}\frac{\partial T}{\partial y}\bigg|_{y=s-0} = \lambda_{\Sigma s+1}\frac{\partial T}{\partial y}\bigg|_{y=s+0}, \quad T|_{y=s-0} = T|_{y=s+0}, \tag{12}$$

$$\rho^{II}\Pi v^{II}|_{y=y_{BD}} = G|_{y=y_{BD}} = 0, \quad p|_{y=y_S} = p_e, \tag{13}$$

$$[(1-\Pi)\sigma_y - \Pi p]|_{y=y_S} = p_e, \quad l|_{y=y_{BP}} = 0. \tag{14}$$

The energy-conservation equation is written in a coordinate system associated with the current position of the PM working surface. Radiant heat transfer in the pores is taken approximately into account by introducing the corresponding components in the effective thermal conductivity: $\lambda_\Sigma = \lambda^{I}(1-\Pi) + (\lambda^{II} + \varkappa(1+\varepsilon)T^3)\Pi$, while the influence of secondary chemical reactions is taken into account by including thermal effects in the total (Q_Σ) thermal effect of the physicochemical processes.

In order to solve the system in Eqs. (1)-(14), it is necessary to add a closing relation for the porosity, gas permeability, and degree of completion of pyrolysis. The formula for the porosity is obtained from the mass-conservation law of an elementary volume of material, taking account of its deformation on swelling and the change in density of the body

$$\Pi = 1 - \frac{\rho_0[1 - \chi(1-K)]}{\rho^{01}(1+\varepsilon)}.$$

The following expression is used for the mathematical approximation of the kinetics of pyrolysis

$$\chi = \begin{cases} 0, & T \leqslant T_{BD}, \\ A_F \operatorname{arctg}\,[m_K(T - T_m)] + B_K, & T_{BD} < T < T_{ED}, \\ 1, & T \geqslant T_{ED}. \end{cases}$$

The gas permeability is calculated from the modified Kozeny–Carmen formula $k = k_0(k_C\Pi)^3/(1 - k_C\Pi)^2$, in which k_C is the clearance coefficient determining the proportion of open, communicating pores in the total porosity Π ($0 \leq k_C \leq 1$). On the basis of the decomposition mechanism of the swelling materials on heating, it may be concluded that the clearance coefficient depends on the degree of cracking of the heated layer, which is associated with the pressure of the surrounding medium and the stress $\bar{\sigma}$ acting in the plane parallel to the working surface. This dependence may be approximated by the following expression

$$k_C = \begin{cases} 1 - \left[1 - k_{C0}\left(\frac{p_e}{10^5}\right)^{-\nu}\right]\exp(-N\bar{\sigma}), & \bar{\sigma} > 0,\ T > T_{EP}, \\ k_{C0}\left(\frac{p_e}{10^5}\right)^{-\nu}, & T < T_{EP} \text{ or } \bar{\sigma} < 0, \end{cases}$$

where k_{CO}, ν, and N are empirical coefficients. According to this expression, the clearance coefficient is small in the plastic region, and increases sharply on passing to the carbonized layer.

The problem may be significantly simplified if the following scheme of change in clearance coefficient is adopted: discontinuous growth at the boundary $y = y_{EP}$ with temperature T_{EP} from zero values in the plastic region to values close to unity in the carbonized layer (Fig. 1a). This schematization corresponds to the case of totally closed pores in the plastic region and pronounced cracking of the carbonized layer. The need to determine the gas permeability of the heated layer vanishes in this case.

In addition, with sufficient accuracy for practical purposes, the velocity of motion of the body on swelling may be regarded as negligibly small in comparison with the flow velocity of the volatile pyrolysis products. Taking this into account, the formula for the pressure in the plastic region may be obtained on the basis of the equation of mass conservation, Eq. (2), and the equation of state of the pyrolytic gases, Eq. (4), in the following form

$$p = \frac{p_*(T)}{\Pi(1+\varepsilon)},\quad p_*(T) = \frac{1}{M}\rho_0(1-K)\chi RT.$$

An expression for the mass velocity of the pyrolytic gases may be found by integrating the equation of mass conservation with respect to the coordinate from the boundary of the plastic region to the surface of the material; taking account of the opening of closed pores of the plastic region as the boundary moves at the velocity $\dot{y}_{EP} = dy_{EP}/dt$

$$G = \rho_0(1-K)\int_{y_{EP}}^{y}\frac{1}{1+\varepsilon}\frac{\partial\chi}{\partial t}dy + \Pi_{EP}(\rho^{II}|_{y_{EP}+0} - \rho^{II}|_{y_{EP}-0})\frac{dy_{EP}}{dt}.$$

In this case, the rate of displacement of the isotherm $T = T_{EP}$ is determined from the obvious relation

$$\dot{y}_{EP} = \frac{\Delta y}{\Delta t}\frac{\Delta T}{\Delta T} = \left(\frac{\Delta T}{\Delta t}\Big/\frac{\Delta T}{\Delta y}\right)\Big|_{y=y_{EP}}.$$

An expression for the pressure when $y_S \leq y \leq y_{EP}$ is obtained on integrating Eq. (3) and taking Eq. (4) into account

$$p = \left(p_e^2 + \frac{2\mu^{II}R}{M}\int_{y_S}^{y}\frac{GT}{k}dy\right)^{1/2}.$$

The formula for the stress arising in the body of the plastic region under the action of the pressure difference is obtained from Eqs. (3) and (5), taking account of the smallness of the mass force $\sigma_y = (\Pi p - p_e)\cdot(1-\Pi)^{-1}$. Using the expression for p in terms of $p_*(T)$, σ_y is obtained in the form

$$\sigma_y = \frac{p_* - p_e}{\varphi} - \frac{p_e}{\varphi}\varepsilon,\quad \varphi = \frac{\rho_0}{\rho^1}[1 - \chi(1-K)].$$

Invariance principles, questions of the correctness of the given model, etc., are considered in accordance with the hypotheses of [2, 3].

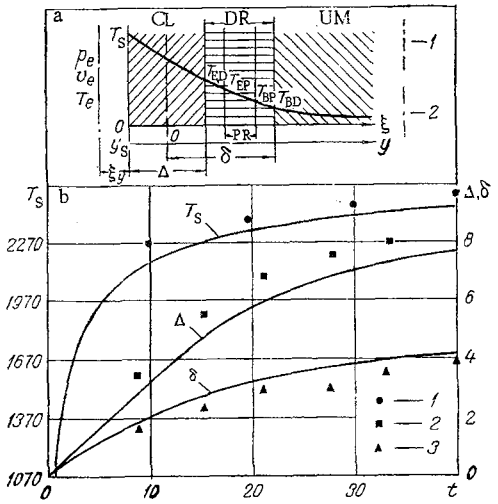

Fig. 1. Calculation scheme (a) and dependence of the surface temperature, coke-layer thickness Δ, and destruction depth δ on the heating time (b): a) CL, carbonized layer; DR, PR, decomposition region, plasticity region; UM, undecomposed material; 1, initial position of PM surface; 2, its position when $v^{ch} = 0$; b) experimental data for the surface temperature (1), coked-layer thickness (2), and destruction depth (3) obtained in an oxygen–acetylene torch for a resinous PM based on phenol-formaldehyde binder at atmospheric pressure, under the conditions: T_e = 2700°K; $\alpha \sim 500\ W/m^2 \cdot °K$; $T_0 = 290°K$; $L_{10} = 0.8 \cdot 10^{-2}$ m, T_S, °K; Δ, δ, mm; t, sec.

The nonlinear system in Eqs. (1)–(14) is solved numerically by computer by a procedure analogous to [4], including an implicit four-point conservative difference scheme for continuous calculation of the "canopy," the simplest difference analogos of Eqs. (9) and (10) in combination with grid densification close to the boundaries, the organization of the iterative process in each time layer with linearization of Eqs. (9) and (10) (isolation of a "cube" at T_S in the radiative component), and averaging of the iterations. By these means it was possible not only to eliminate the difficulties arising on approximating boundary conditions of the third kind (especially in the presence of radiant heat transfer) with second-order accuracy by the method of [5] and the associated appearance of a minus sign in the fitting coefficients at $d\lambda/dt < 0$, but also to ensure the same order of accuracy of the approximation and to reduce the number of iterations.

The computational algorithms for determining the position of the moving boundaries of the plasticity and decomposition regions, the external PM boundaries on swelling, and the chemical (surface) mass loss are constructed on the basis of the theory of [6]. The calculation of the motion of the external boundaries of the deformed material is based on the determination of l at i grid points and its transformation according to the scheme $h_i^{\gamma} = h_i^{n-1} + l_i^{\gamma}$, leading to displacement of the boundaries through a distance

$$y_*^{\nu} = \sum_i l_i^{\nu} = \sum_i \int_{y_{BP}}^{y} \ln(1+\varepsilon_{yi}^{\nu})\,dy,\quad \varepsilon_{yi}^{\nu} = \varepsilon_{yi}^{n-1} + \Delta\varepsilon_{yi}^{\nu},\quad l_i > 0,$$

$$\Delta\varepsilon_{yi}^{\nu} = A_{\varepsilon}(\sigma_{yi}^{\beta})^{\nu}\,\tau_n^{r}\exp\left(-\frac{B_e}{(T_i)^{\nu}}\right),\quad T(y_*,\ t) = T(y_S,\ t),\quad \nu = J(\text{or}\quad n),$$

$$T[y_i^{\gamma},\ t_n] = T[(y_{i-1}^{n-1} + h_i^{n-1} + l_i^{\nu}),\ t_n],\quad h_i = y_i - y_{i-1},\quad \tau_n = t_n - t_{n-1},$$

n, j = 1, 2, ... are the numbers of time layers and iterations; i = 1, 2, ... ; $y_{EP} \le y \le y_{BP}$. The position of the boundaries of the regions of internal decomposition and plasticity is determined from the temperature profile in the PM and the isotherms ($T = T_{BD}$, T_{BP}, T_{EP}, T_{ED}) by explicit derivation of the boundaries of interpolation. The motion of the external PM boundaries with chemical entrainment is calculated by the method of [6].

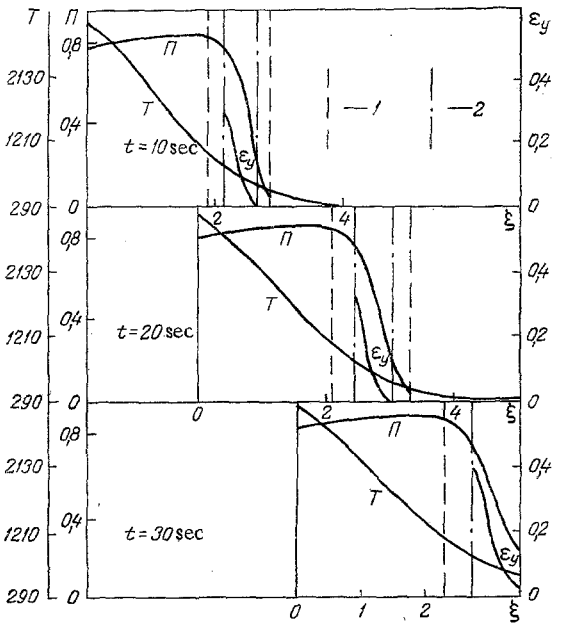

Fig. 2. Distribution of the temperature, porosity, and relative deformation over the PM thickness and time: 1) DR; 2) PR. T, K; ξ, mm.

The thermophysical and thermochemical characteristics of the materials required for numerical calculations are determined as a result of special experimental investigations. The values of ρ_0, c_p^I, λ^I are obtained on completely coked samples ground to a powder. The thermal conductivity, specific heat, and viscosity λ^{II}, c_p^{II}, μ^{II} of the volatiles are calculated from their composition; the kinetic parameters m_k, T_m, A_k, B_k, K of thermal decomposition are determined from thermogravimetric curves by solving the identification problem. The thermal effect of thermal decomposition is calculated in accordance with the Hess law from the heat of formation of the initial material and its decomposition products. The rheological parameters of materials in the plastic zone are found from the creep curves.

A series of parametric calculations have been performed on an ES-1055 computer for a two-layer plate, with the first layer (s = 1) swelling, using the characteristics obtained and a Fortran program developed on the basis of the computational algorithms and principles of construction of applied programs of packet [4]; the basic results are shown in Figs. 2-4.

Comparison of experimental data and the results of calculation (Fig. 1b) indicates that they are in good agreement (the maximum discrepancy obtained for Δ is no more than 15%), which, like the convergence of difference solutions established by the method of [6], confirms not only that the assumptions adopted in solving the problem are correct but also that the computational algorithm developed is reliable.

The distribution of the temperature, the porosity, and the relative deformation of the material over the thickness of the swelling PM at various times is shown in Fig. 2. It follows from an analysis of the curves, in particular, that the relative deformation has a maximum at the boundary of the plastic region with temperature T_{EP} and the porosity has a maximum at the boundary between the decomposition region and the carbonized layer; their maximum values increase with time. The temperature profile in the plasticity region is deformed (straightened) on account of swelling of the plastic-region body in the direction of the PM working surface and decrease in the heat conduction as a result of the increase in porosity.

The temperature $T(L_{s=1})$ at the boundary between the first and second layers in the presence of swelling and surface entrainment of the PM mass decreases from 628°K (without swelling) to ~580°K (t = 30 sec), i.e., by ~50°K. As a result of the calculations, it is established that this difference in $T(L_1)$ increases approximately threefold with 50% decrease in M: $T(L_1)$ = 490°K. In the absence of entrainment, $T(L_1)$ = 320°K, i.e., swelling of the PM, leading to "blocking" of the heat-propagation process (on account of increase in II), reduces $T(L_1)$ by half (or more, depending on the intensity of swelling).

Thus, swelling leads to significant increase in porosity close to the internal boundary of the carbonized layer and reduction in temperature at the boundary between the layers.

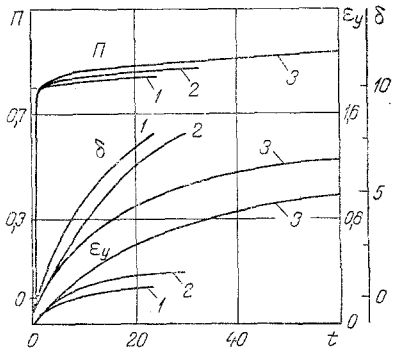

Fig. 3

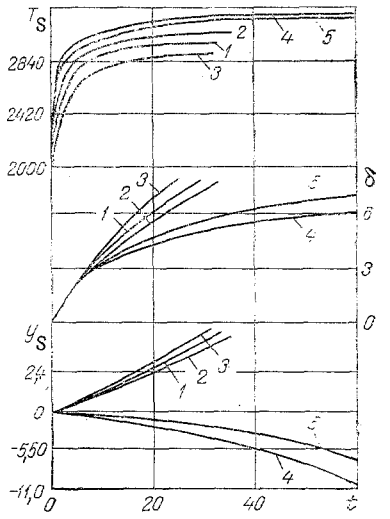

Fig. 4

Fig. 3. Change in porosity, destruction depth, and relative deformation over time, with various heat-transfer conditions: 1) $v_e = 200$ m · sec^{-1}, $\alpha = 500$ W/m^2 · °K; 2) 100, 289; 3) 10, 46.

Fig. 4. Dependence of the surface temperature, destruction depth δ, and PM coordinate y_S on the time, molecular weight of the volatile components, pressure, and surface entrainment of mass: 1) M = 100; 2) 50 kg/mole; 3) calculation in the absence of swelling; $p_e = 0.1$ MPa, b = 0.23; 4) $p_e = 0.1$; 5) 4 MPa; M = 100 kg/mole; $G^{ch} = 0$ (no entrainment). T_S, °K; δ, y_S, mm; t, sec.

The dependence of the destruction depth (up to 573°K), maximum porosity, and relative deformation on the heating time, velocity of the external flux, and convective heat-transfer coefficient are shown in Fig. 3. With increase in flux velocity, the heat-transfer coefficient and value of Π increase, while ε_y decreases (curves 1, 2) on account of more rapid progress of the front $y = y_{BD}$ (or increase in the destruction depth δ) with increase in α (curves 1-3 for δ). With completion of the process of PM destruction, the calculation stops.

The influence of swelling, chemical entrainment, and pressure in the external gas flow on the PM surface temperature, its destruction depth, and the coordinate y_S of the PM working surface (relative to its initial position) is shown in Fig. 4. Pressure leads to reduction in intensity of swelling. Whereas the sample size (L_1) increases by approximately 125% by the 60th second at $p_e = 0.1$ MPa (curve 4 for y_S), the increase in the thickness at $p_e = 4$ MPa is no more than 80% (curve 5). With increase in pressure and molecular weight of the gaseous thermal-decomposition products, and in the presence of surface entrainment of mass, the "blocking" of heat on swelling is reduced (the porosity is decreased). As a result, there is a decrease in PM surface temperature, and δ increases (curves 1, 2, 4, 5 for T_S and δ).

It is evident from Fig. 4 that, with the chosen heating conditions, swelling decreases the destruction depth of the material to 25% (curves 1-3).

The present investigations show that swelling must be taken into account in calculating the temperature fields in PM, since they lead to change in character of the heat propagation in the material and, as a consequence, to considerable decrease in heating depth.

NOTATION

t, ξ, y, L, time, transverse coordinates associated with the current and initial positions of the PM surface, and thickness; T, temperature; I, enthalpy; p, pressure; v, velocity; G, mass velocity; a, sound velocity; α, η, A_{ef}, coefficients of heat transfer, injection, and radiational properties; λ, c_p, ρ, thermal conductivity, specific heat, and density; Q, thermal effect; K, coke number; m_F, η_M, mass fraction of filler in the initial material and chemicomechanical crumbling of coke residue defined according to [2]; b, oxidative potential; χ, degree of thermal decomposition; M, μ, molecular weight and viscosity of pyrolytic gases; R, universal gas constant; Π, porosity; k, k_C, permeability and clearance coefficient; F, mass force; σ, stress; ε_y, ε, relative

and bulk deformation; l, displacement; A_ε, B_ε, kinetic parameters of deformation; σ', Stefan–Boltzmann coefficient; $\varkappa$, empirical coefficient; h, τ, difference-grid steps over the coordinate and time. Indices: 0, initial; e, external gas flow; S, surface; ch, chemical entrainment; I, condensed phase (body); II, gas phase in material; s, layer number; Σ, total; BD, m, ED, beginning, maximum, and end of decomposition; BP, EP, beginning and end of plastic state.

LITERATURE CITED

1. V. F. Zakharenkov and L. I. Shub, "Temperature fields in thermoprotective materials," Inzh.-Fiz. Zh., 25, No. 5, 827-836 (1973).
2. B. M. Pankratov, Yu. V. Polezhaev, and A. K. Rud'ko, Interaction of Materials with Gas Flows [in Russian], Mashinostroenie, Moscow (1976).
3. G. V. Vinogradov and A. Ya. Malkin, Polymer Rheology [in Russian], Khimiya, Moscow (1977).
4. N. G. Chubakov, "Solving nonsteady nonlinear boundary problems of heat and mass transfer in regions with mobile boundaries," in: GFAP Information Bulletin: Algorithms and Programs [in Russian], No. 4, VNTITs, Moscow (1980), p. 22.
5. A. A. Samarskii, Theory of Difference Schemes [in Russian], Nauka, Moscow (1977).
6. N. G. Chubakov, "Difference method of solving one class of nonlinear boundary problems of heat and mass transfer in regions with mobile boundaries," Inzh.-Fiz. Zh., 42, No. 3, 491-492 (1982).

VARIATIONAL ESTIMATE OF THE EFFECTIVE GENERALIZED CONDUCTIVITY TENSOR OF A TWO-PHASE MEDIUM WITH AN ANISOTROPIC DISTRIBUTION OF PHASES

V. P. Kazantsev

UDC 536.24

An inequality is found for the effective generalized conductivity tensor of a two-phase medium with an anisotropic distribution of phases.

There are a large number of calculations of the effective generalized conductivity of a two-phase inhomogeneous medium; see for example [1-3]. The idea of a generalized conductivity derives from a local coupling of two vectors fields (denoted by **E** and **j**) by a linear relation with the proportionality factor dependent on the material characteristics. In the absence of sources, one of the fields will be potential, and the other solenoidal, and the equations for the spatial distribution of fields will be given by

$$\mathrm{rot}\,\mathbf{E} = 0;\ \mathrm{div}\,\mathbf{j} = 0;\ \mathbf{j} = \Lambda\mathbf{E}, \tag{1}$$

where the generalized conductivity will in general be a tensor of the second rank. In the present paper we consider the case of a scalar $\Lambda > 0$ which is more often encountered in practice.

The set of equations (1) describes processes of heat conduction, diffusion, electrical conduction and also the electric field distribution in a dielectric and the magnetic field in a material with the magnetic permeability differing from unity. In the particular case of heat conduction, **E** is the temperature gradient and **j** is the heat flux; then Λ will be the thermal conductivity.

Various methods have been used to calculate the effective conductivity. The variational method has been used in only a relatively few cases, as can be seen in the reviews [1-3]. However, variational methods have several advantages which show considerable promise. For example we show that the variational inequality obtained here yields not only an approximate effective generalized conductivity but also allows calculation of

Krasnoyarsk State University.

Translated from Inzhenerno-Fizicheskii Zhurnal, Vol. 45, No. 3, pp. 480-487, September, 1983. Original article submitted April 27, 1982.

0022-0841/83/4503-1060$07.50